ADVANCED PHYSICS RESEARCH Open Access
www.advphysicsres.com

Homologous Self-Assembled Superlattices: What Causes their Periodic Polarity Switching?

*Varun Thakur, Dor Benafsha, Yury Turkulets, Almog R. Azulay, Xin Liang, R. S. Goldman, and Ilan Shalish**

Quantum semiconductor structures are commonly achieved by bandgap engineering, which relies on the ability to switch from one semiconductor to another during their growth. Growth of a superlattice is typically demanding technologically. In contrast, accumulated evidence points to a tendency among a certain class of multiple-cation binary oxides to self-assemble spontaneously as superlattice structures. This class is dubbed the homologous superlattices. For a famous example, when a mixture of indium and zinc is oxidized, the phases of In-O and ZnO separate in an orderly periodic manner, along the ZnO polar axis, with polarity inversion taking place between consecutive ZnO sections. The same structure is observed when the indium is replaced with other metals, and perhaps even in ZnO alone. This peculiar self-assembled structure is attracting research over the past decade. The purpose of this study is to gain understanding of the physics underlying the formation of this unique structure. Here, an explanation is proposed for the long-standing mystery of this intriguing self-assembly in the form of an electrostatic growth phenomenon and a test of the proposed model is carried out on experimental data.

1. Introduction

Much of the work on transparent conductive oxide semiconductor thin films and nanostructured devices has focused on zinc oxide[1–5] or ZnO-based compounds, namely In-Ga-Zn-O, Zn-Sn-O, and In-Zn-O.[6–8] The general consensus behind choosing ZnO-based structures seems to be that for obtaining transparent materials with high conductivities, a class of oxides with multiple cation species with the electronic configuration of $(n-1)d^{10}s^0$ holds the most promise.[9] The empty metal cation s-orbitals generally form the conduction band in these materials, while the overlap between them gives the n-conduction pathway, making their electronic configuration most suitable for various device applications.

Among the ZnO-based semiconductor-oxides, In-Zn-O has received special attention for an interesting phenomenon. Thin films of In-Zn-O were observed to possess a superlattice structure following the relation $In_2O_3(ZnO)_m$ and were therefore considered to be a homologous series.[10] This unique structure holds a special interest due to the spatial confinement of conduction electrons in 2D layers, affording them exceptional electron transport properties in addition to their being excellent transparent oxide semiconductor materials.[11,12] In 2003–2004, Nomura et al. demonstrated transparent field effect transistors fabricated on a complex $InGaO_3(ZnO)_5$ superlattice structure which showed excellent properties including a carrier mobility of 80 $cm^2\ V^{-1}\ s^{-1}$, turn on voltage of −0.5 V, and an on-off ratio of 10^6.[13–15] Following this demonstration, other groups became engaged in fabrication of transistors using In-Zn-O[16–19] and Sn-Zn-O,[20,21] In-Ga-Zn-O,[22–26] and Al-Zn-O.[27] Field effect mobilities ranging from 5 to 50 $cm^2\ V^{-1}\ s^{-1}$ depending on annealing temperatures were reported with turn on voltages between −5 and 15 V.[20] Devices fabricated by Dehuff et al.[16] also showed excellent properties with mobilities reaching 55 $cm^2\ V^{-1}\ s^{-1}$ and turn on voltages ≈–20 V. Research has also been carried out on applications such as photocatalysis.[28] These papers mark the onset of intense research of these self-assembled ZnO-based superlattice structures for various electronic, optoelectronic, and thermoelectric applications. In the following years, several papers reported materials possessing the general electronic configuration of $(n-1)d^{10}s^0$ $(n \geq 4)$, among which the

V. Thakur, D. Benafsha, Y. Turkulets, A. R. Azulay, I. Shalish
School of Electrical Engineering
Ben-Gurion University
Beer Sheva 8410501, Israel
E-mail: shalish@bgu.ac.il
X. Liang
Beijing Institute of Nanoenergy and Nanosystems
Chinese Academy of Sciences
Beijing 101400, China
X. Liang
School of Nanoscience and Engineering
University of Chinese Academy of Sciences
Beijing 100049, China
R. S. Goldman
Department of Materials Science and Engineering
University of Michigan
2300 Hayward, St., Ann Arbor, MI 48109, USA

The ORCID identification number(s) for the author(s) of this article can be found under https://doi.org/10.1002/apxr.202300039

DOI: 10.1002/apxr.202300039

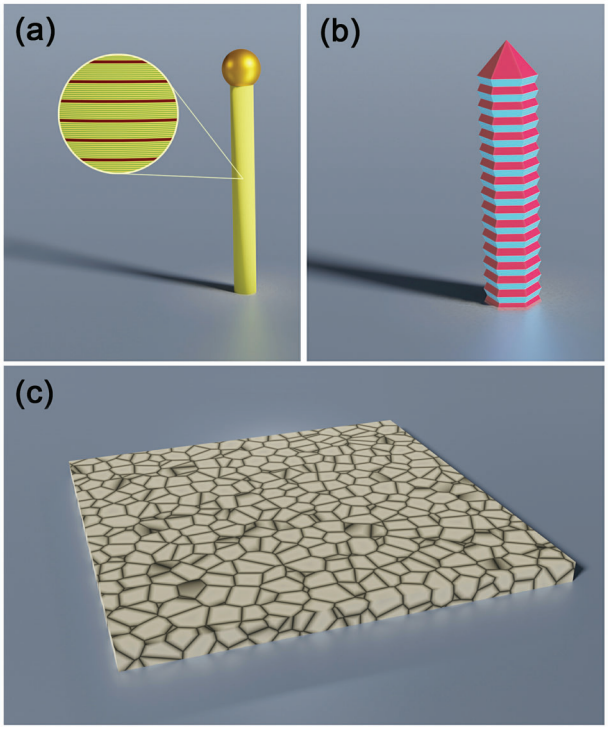

Figure 1. The ZnO-based homologous crystal structures are commonly observed as a) nanowires, b) nanorods, and c), polycrystalline layers. They are easily identifiable in nanorods by the corrugated surface caused by the periodically inverted domain layers. However, this surface structure is typically missing in nanowires. This is probably for the same reason that crystal facets are only observed in thick enough wires.

most common superlattice structures were those observed in Zn-Sn-O, In-Zn-O, and Ga-In-Zn-O.

While there have already been published reviews mentioning the superlattice structure, they have not focused on the main mechanism of its formation.[29] In the most commonly studied of these materials, In-Zn-O, the ZnO flips its polarity periodically along the polar axis, while the indium may be viewed as a polarization-inversion promoter. Explanation of the causes for the formation of periodic polarity switching is currently still missing. We propose here a simple electrostatic model that explains the phenomenon as a periodic charging process taking place during the crystal growth, due to the strong polar nature of the main material. Our model and results emphasize the important role of electrostatics in the growth of polar semiconductors—a mechanism of which the semiconductor material community has mostly been unaware.

Already at an early stage, In-Zn-O compound crystals were identified to occur at specific sequences of layers that led to their classification as inorganic homologous series. Sections of m monolayers of ZnO were found to be periodically sandwiched between monolayers of the structure $InMO_3$, following the formula $InMO_3(ZnO)_m$ (where M = In, Fe, Ga, Al, m = integer). Interestingly, the layers self-assemble to form this ordered periodic sequence of alternating phases and do so both in films, and in nanowires (**Figure 1**).

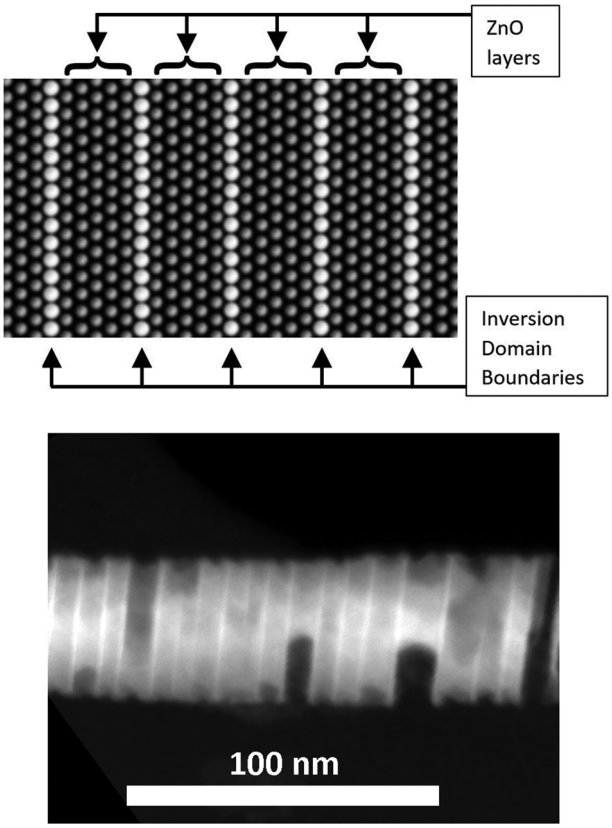

Figure 2. Top—An illustration showing the typical structure revealed in transmission electron microscope image: slabs of several (m) ZnO layers (here for example $m = 4$) are separated by monolayers of another metal oxide. The polarity of each ZnO slab is inverted relative to those of its neighboring slabs, so that the other metal oxide monolayers form inversion domain boundaries. Images of similar structures have been shown, for example, by Ohta et al.,[11] Guo et al.,[35] Park et al.,[36] and by Cao et al.,[37] Bottom—TEM image of In-Zn-O nanowire. The bright lines traversing the wire mark the In-O inversion domain boundaries.

Initial observations of these structured materials were made in ceramic polycrystalline thin films. Synthesis of what was thought to be $In_2O_3(ZnO)_m$ (m = 2–5 and 7) having a layered wurtzite structure was first reported in 1967 by Kasper.[30] However, two decades elapsed before the first attempt by Cannard and Tilley in 1988 to analyze the structure using high resolution transmission electron microscopy (TEM).[31] They reported the presence of metal-oxygen layer stacks perpendicular to the c-axis in the hexagonal crystal system. Their seminal study gave an important insight into the actual atomic order in this superlattice. Nakamura et al. then synthesized and analyzed the phase relations in the In_2O_3-$ZnGa_2O_4$-ZnO system at 1350 °C and proposed homologous phases having solid solutions of $(InGaO_3)_2ZnO$, $In_{1.33}Ga_{0.67}O_3(ZnO)$-$InGaO_3(ZnO)$-$In_{0.92}Ga_{1.08}O_3(ZnO)$, $In_{1.68}Ga_{0.32}O_3(ZnO)_2$-$InGaO_3(ZnO)_2$-$In_{0.68}Ga_{1.32}O_3(ZnO)_2$, and $In_2O_3(ZnO)_m$-$InGaO_3(ZnO)_m$-$In_{1-x}Ga_{1+x}O_3(ZnO)_m$ (m = 3–13)($0<x<1$).[32]

Following studies established that the $In_2O_3(ZnO)_m$ system is comprised of InO^{2-} and $(ZnO)_m$ layers alternating along the c-axis of the wurtzite crystal system (**Figure 2**).[33] To confirm this

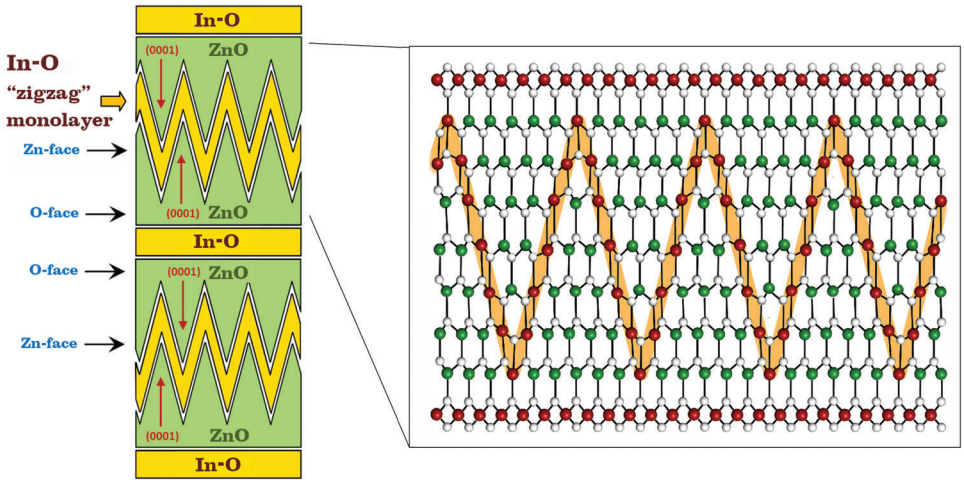

Figure 3. Illustration of the In-Zn-O superlattice structure, where each ZnO slab has an opposite polarity to its neighboring slabs, and the boundaries between the slabs are flat on the O-face and zigzagged on the Zn-face. Three decades elapsed before the zigzag boundary structure was realized. During this time the two ZnO slabs neighboring the zigzag layer were thought to be a single In-Zn-O ternary layer. Part of the difficulty may be related to the fact that the zigzag boundary are not always present and sometimes are replaced with an planar In-O layer.

finding visually, several groups carried out high resolution TEM imaging with electron diffraction. High resolution TEM studies by the Kimizuka group showed the presence of a modulated, zigzag, structure, which was absent in the results of Cannard and Tilley, because of the higher m values of their structures.[34]

The finding of the zig-zag structure was an important step toward the understanding of the structure, because it previously led to the wrong conclusion that the In was part of a ternary In-Zn-O phase, whereas now, it became clear that some of the previously assumed ternary phases were actually two inverse-polarity ZnO domains with an In-O decorating the zigzag boundary.

Based on Z-contrast scanning tunneling electron microscopy imaging, Yan et al. suggested the presence of a polytypoid structure.[38] Their results provided a crucial insight into the structure of $In_2O_3(ZnO)_m$ films, where irrespective of the m value, the number of ZnO layers between each In-O layer was found to be inconsistent. In other words, the structure along the c-axis had variable periodicity. Further, the analysis of the Z-contrast image to ascertain the complete structure also revealed that the In-O layer containing O atoms in an octahedral position form a wurtzite structure with the Zn atoms below, necessitating an inversion of polarity in the ZnO slab following the In-O layer. This was also the first report of the In-O layers forming an inversion domain boundary in the $In_2O_3(ZnO)_m$ structure. Since each ZnO slab is bound by two In-O layers, the ZnO layer itself must contain another domain boundary. This other domain boundary was named by the authors a "mirror domain boundary." In that study, this domain boundary was not observed to be zigzagged.

The finding of periodically alternating polarities was a major leap in the understanding of the structure. This realization was delayed for a long time due to the inconsistent occurrence of the zigzag shape at one of the domain inversion boundaries (**Figure 3**). As long as this zigzag boundary had not been realized to be a boundary, it was thought that the material between two flat boundaries was a solid solution InZnO ternary. We note here that the structure closely resembles that of periodically twinned ZnO. However, twinning is only one of three types of this boundary, with the other two types being the flat mirror boundary (not twinning) and the zigzag boundary, which structure has yet to be fully understood. The decoration of the inversion domain boundaries with the other metal has also been misleading as it does not always take place in the same manner. In the mirror boundary indium just replaces Zn, while in the twin boundary they form an In-O structure. Several theoretical studies following the discovery of the zigzag boundary were undertaken to explain why this modulated boundary was energetically favorable.

As of the year 2000, and following the buildup of interest in nanowires, structural analysis was made easy. Nanowires do not require the laborious preparation of TEM cross-section layers. Their structure itself provides a ready-made TEM cross-section sample. No small advantage was the fact that at no additional complexity, one could easily grow a superlattice nanowire at a time when much effort was invested into adding various functionalities to the new "nanotechnology building block." From this point and on, most of the studies were carried out on nanowires.

The first report of $In_2O_3(ZnO)_m$ nanowires was by Jie et al.[39] They observed the formation of the superlattice structure only in a part of the substrate area (20–40%). High resolution TEM images and corresponding selective area electron diffraction (SAED) patterns revealed the presence of a superlattice, reflected as a series of smaller diffraction spots between two adjacent main spots (commonly dabbed "streaking").

The relative ease of obtaining superlattice nanowires by self-assembly ignited the imagination of many researchers in the field, and expectations for superior devices based on these structures motivated several device studies. Several groups doped In-Zn-O nanowires with elements such as Sn, Si, etc., in an attempt to improve the material properties, such as electron mobility. One such report was by Na et al. in 2005, who reported synthesis of Sn-doped $In_2O_3(ZnO)_4$ and $In_2O_3(ZnO)_5$ superlattice nanowires.[40] The atomically-resolved high resolution TEM image of a nanowire revealed the polarity inversion between adjacent ZnO slabs with In-O layers acting as inversion domain boundaries. In 2006, Xu et al. reported the synthesis of

In-Zn-O nanowires, where some of the nanowires showed periodical twinning structures.[41] The authors did not observe such twinning in ZnO alone and this led them to surmise that the introduction of In into the lattice is the cause for the observed twinning. Many of the papers on In-Zn-O nanowires report studies of synthesis.[39,42–53] Some report similar observation in nanobelts,[54–61] as well as several other nanostructures.[49,62–65]

Attempts to diversify the material choice started already with the early ceramic thin film studies. The wide interest in superlattice nanowires attracted further research that naturally explored other materials in the hope to increase the material choice and engineer certain material properties. Since the In-Zn-O system has been the easiest venue to obtain the superlattice, many of the studies only slightly perturbed that system by introducing "doping" of additional metals. This so-called "doping" was typically at the percent range rather than the part-per-billion that is typical of semiconductor doping. In many of these cases, the zigzag boundary is still observed. However, in some of the cases the boundaries are typically flat while the periodic polarity inversion is common to all of these systems.

The smallest perturbation to the In-Zn-O system was perhaps the addition of another group III metal to the In, or a replacement of the In by another group III metal.[32,66] More significant perturbations were the replacement of In with other metals, such as Cd, Sb, or Sn.[36,37,67]

As previously discussed, these homologous self-assembled superlattice structures have been found to be consisted of periodic sequences of polarity-inverted domains, where each section is, in principle, identical to its two neighboring sections, except for its inverted polarity. Several reports suggest that periodic polarity inversion does not necessarily require the presence of another metal, as it has been also observed in undoped ZnO,[68] as well as in other undoped binary wurtzite crystals, e.g., ZnS,[69] and SiC,[70,71] where it is commonly referred to as periodic twinning.

Theoretical studies of these superlattices mainly address two general aspects: Crystallographic structure, and electrical/optical properties. All these works take as granted that the ZnO flips its polarity in a periodic manner and that the other metal is found at the inversion domain boundaries. The structural studies mainly address the formation of the zigzag boundary and convincingly model its formation using structural energy considerations.[33,35,72–77] Given the polarity inversion, calculation shows that the inversion boundaries minimize the energy of the In-O and hence explains the presence of In-O at the boundaries, but the question has remained: What causes the periodic inversion in the first place?

In this paper, we attempt to explain the physics underlying the spontaneous formation of the so-called homologous compound superlattice structures.

2. Model

In this section, we build upon the foundations laid by the above-reviewed accumulated knowledge to propose a mechanism to explain the observed self-assembly of the homologous superlattices. To enable electrostatic effects on crystal growth, the crystal has to be able to interact with electric charges or electric fields. Such interaction has been reported by some of the authors of this paper[78,79] and by others[80] for wurtzite materials. Wurtzite

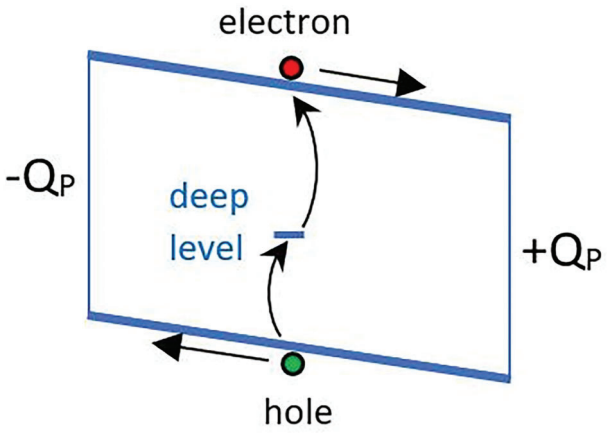

Figure 4. Band diagram of a single period of the periodic alternating-polarity structure. A single period of, e.g., ZnO, has opposite polar charges on its ends that give rise to a built-in field. The typically high temperature of the growth increases the probability of thermal generation, especially if mid-gap states such as deep levels and surface states are available and reduce the minimal energy required for band-to-band generation. The generated electron–hole pair is then separated by the built-in field. Another source of energy, much stronger than the phonons, are photons emitted as incandecent glow during the growth.

crystals have a built-in electric field that can interact with mobile electric charges. This field is a natural trait of the wurtzite structure, a result of its spontaneous polarization. For example, ZnO nanowires often grow vertically-aligned on SiO_2 substrates. SiO_2 is amorphous, and thus cannot provide epitaxial guidance to align the wires. Nonetheless, the ZnO wurtzite lattice has an intrinsic built-in electric field, and it was shown that the interaction of this field with the field emanating from parasitic charge in the SiO_2 causes the alignment of the polar axis of the crystal with the external field. When the sign of the electric charge in the SiO_2 was changed, the polar axis of the wires flipped over.[78] These observations showed an electrostatic effect of substrate charge. However, the same mechanism could be in effect at each inversion domain boundary along a periodically polarity-inverted wire. All that is required is that during the growth of each section, mobile electric charge will gradually accumulate at the growth edge until, at a very specific length, it will build up a strong enough electric field to cancel the effect of the polar charge at that face and thereby to enable the flip over of the polarity of the next section. The same process would then reiterate in the next section and so on and so forth. The crystal's polar built in electric field separates mobile charges along the growth axis in a way that charges of one sign float to the growth edge, while charges of the opposite sign are swept downward (**Figure 4**).

Let us denote the In in the In-Zn-O as the secondary cation. The secondary cations observed in the homologous superlattices usually do not form oxides that have spontaneous polarization. It seems that for this reason, they have higher likelihood to attach to the growth surface, once the polar charge is fully screened out by mobile charge. When they do, their bond angles allow them to bridge over efficiently to the inverted phase that starts to grow immediately on top of them.

Some of the inversion boundaries are flat (when an O-face is facing an O-face) and some of them are zigzagged (Zn-face to

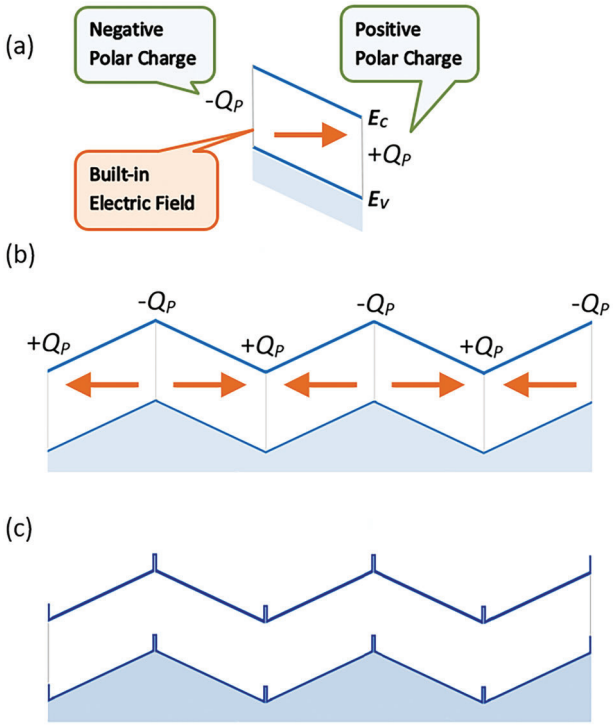

Figure 5. Qualitative electronic band diagrams of an In-Zn-O homologous superlattice. a) A single ZnO section—the intrinsic polarity induces a built-in electric field that tilts the bands. b) Periodically twinned ZnO—essentially possesses a band structure that is similar to n-i-p-i superlattice consisting of an alternating series of triangular potential wells and triangular barriers. The built-in electric field in each section has an opposite direction than the fields in the two adjacent sections. c) In-Zn-O—if the added indium were In_2O_3 it would probably create an off set quantum size layer as shown. In reality the layer is InO_2, but according to photoluminescence studies, the offset is more or less the same.

Zn-face boundaries are zigzagged in some of the cases). A similar zigzag inversion boundary has been reported in InN and ZnO nanorods.[79] In those systems, there were no secondary cations, and the transition took place over much longer sections of the order of more than a micrometer. The mechanism proposed there was a symmetric nonuniform distribution of mobile charge causing inversion only at the highly charged points in the structure. At this time, we cannot explain why there would be such a fundamental difference in the mobile charge distribution between the two polar faces of the homologous superlattice system. However, the mechanism of mobile-charge-induced polarity-inversion is definitely in line with the present model.

There could be two major sources for electron–hole thermal generation: in the bulk, and/or on the surface. Thermal generation seems likely during crystal growth as the growth temperature is typically high. However, direct band-to-band excitation is less likely in a wide gap material as is ZnO then in e.g., GaAs. To account for generation in wide gap materials such as ZnO, we have to consider an indirect excitation through deep-levels (**Figure 5**). Deep levels at surfaces (surface states) typically span wide energy ranges (e.g., the yellow luminescence band in GaN,[81] or the green luminescence band in ZnO[68]) making them the more probable route for generation.

The amount of charge generated in each wire section should be relative to its volume, if the charge is generated in the bulk of the material, and should be relative to its surface area if the surface is the source. Whether it is this way or the other, the rate, at which the charge will be accumulated, has to increase with the wire radius, because both the surface area and the volume increase with the wire radius. If such charging mechanism is indeed at work, this would predict a dependence of the section length on the wire diameter. The exact nature of this dependence, however, should vary with the relative part of each of the generation mechanisms, surface, or bulk.

In Section 3, we show that experimental data from the literature may be used to test this explanation, and if validated, to also attest the origin (bulk vs surface) of the generation mechanism.

3. Proposed Experimental Test

Understanding of the structure of the ZnO-based homologous self-assembled superlattices has evolved along the years. Nonetheless, no clear idea of what causes the layers to self-assemble the way they do has been put forward so far. While the effect was observed in both polycrystalline films and in nanowires, we choose, for convenience, to start with modeling their formation in nanowires. The reason for this choice will be explained later, when we move on to generalize to include other structures and layers. Currently, we understand that the structure of these self-assembled superlattice nanowires is in fact very similar to that observed in periodically-twinned ZnO nanowires. The ZnO wire is periodically sectioned into identical sections having alternating polarity along the polar-axis of the crystal. Each two consecutive sections are separated by a domain-inversion boundary. In the superlattice version of this structure, an additional metal, or a combination of several metals, forms a monolayer that bridges and connects the two neighboring domains of opposite polarities right at the domain-inversion boundary. Also, in the homologous superlattice, the domain inversion boundary is not always a twinning boundary.

The consecutive sections are typically short (1–100 nm). Since the polar axis is always perpendicular to the inversion boundaries, each of the two ends of each single section has a constant polar charge of opposite sign. These two opposite sheet charges constitute between them a built-in electric field. Due to the short length, this field is typically very strong, tilting the energy bands (Figure 5a) and leaving this section fully depleted. In each section, the field is opposite to the fields in adjacent sections. Hence, a periodically-twinned ZnO nanowire may be viewed as a naturally-formed doping superlattice (Figure 5b), also known as a "n-i-p-i" superlattice structure,[82] where the domain or section boundaries are charged with charges of identical magnitudes and periodically alternating signs. To overcome this endless series of barriers and induce conduction across them would require a very high voltage if at all possible. This suggest that much of the previous studies that carried out transport measurements actually measured conduction at grain boundaries rather than within the grains.

When another metal, e.g., indium, is added to the structure, no ternary phase is formed as long as the In density is small, but rather the other metal forms a single atomic layer (not even a monolayer) that bridges between the two adjacent opposite

polarity slabs of ZnO. Perhaps this other metal may be viewed as a "polarity-inversion-promoter," although periodic-twinning appears to take place also in the absence of the other metal. The presence of this other metal oxide at the domain inversion boundary probably perturbs the energy band line up creating notches, quantum wells and quantum barriers, at the very boundary (Figure 5c), because of the band discontinuity between the ZnO and the oxide formed by the other metal.

We have previously reported the effect of charging and electric fields on the growth direction of polar semiconductors.[78,79] In the case of polar semiconductors, especially ZnO, it appears that the effect of electric fields emanating from charges may sometimes have a stronger effect than epitaxial guidance.[78] If a nanowire of polar semiconductor is growing in the polar direction, fixed polar charge will always be present at the growth end of the wire to guide further growth. However, this fixed polar charge is often partially or totally screened out by mobile charges of the opposite sign.

Let us imagine a nanowire growing along the polar axis. The growth takes place at the upper edge of the wire forming a new section/domain. The growth is carried out at a high temperature. Due to the high growth temperature there is a strong incandescent glow from all the hot surfaces. This radiation gives rise to generation of electron–hole pairs in this upper section as it is formed. The strong built-in polar electric field separates the pairs. Electrons are swept to the end with the positive polar charge, while holes are swept to the end with the negative polar charge. After their life time is over, the charges recombine. The balance between generation and recombination leaves a certain net charge that is swept to the growth edge and cancels some of the fixed polar charge at that end. We will assume that this band-to-band generation takes place in the bulk of the material, and its rate is fixed per unit volume, while in parallel, there is also an indirect generation through bulk deep levels at a fixed rate per unit volume, and an indirect generation through surface states takes place on the side walls of the growing section and its rate is fixed per unit surface area.

As the section grows longer, its volume increases and so does its surface area, though not at the same rate. This brings a gradual growth in the net generation. The growth continues until a critical length is reached, at which the generated mobile charge accumulated at the growth-end totally screens the polar charge. Passing this point induces a flip-over of the growth polarity and an inversion boundary is formed. A new section starts to grow with an opposite polarity, and again, its growth is limited to the same critical length for the very same reason. The flip-over is assisted by atoms of the other metal that can more easily form the slightly different angles between the chemical bonds that are required for the polarity flip-over, but the flip-over may also take place without the other metal, thus forming a periodically domain-inverted homostructure wire rather than the heterostructure superlattice wire.

The above mechanism implies dependence of the section length (the period of the superlattice) on the wire diameter as well. On the other hand, it does not imply any dependence on the type of the other metal or its presence at all.

If we assume a net density of pairs generated (whether directly or indirectly) in the bulk (generation minus recombination) of G_B, then to get the number of generated pairs, we will need to multiply it by the section volume, $\pi R^2 L$, where R is the radius of the wire, and L—the section or period length. Similarly, we will need to assume a net generation at the surface, G_S, and multiply it by the section surface area, $2\pi RL$, to get the number. Adding these two numbers, we get the critical number of charges required to induce a polarity flip-over. This critical number equals a density, C, times the wire cross-section area, πR^2

$$\pi R^2 L G_B + 2\pi RL\, G_S = \pi R^2 C \tag{1}$$

Extracting the section length, L, we get a dependence of the section length on the nanowire radius, R

$$L\,(R) = \frac{C}{G_B}\,\frac{R}{R + 2\frac{G_S}{G_B}} \tag{2}$$

To test the validity of this model, we need data points of (R,L), where each superlattice wire provides a single data point. Fitting the data with Equation (2) should tell us about the ratios among the 3 parameters. Direct generation in the bulk requires that a photon that will be energetic enough to excite an electron over the bandgap. In the case of ZnO the bandgap is 3.3 eV. At the absence of ultraviolet photons, the probability for this transition should be low. In contrast, deep levels, whether on the surface or in the bulk situated somewhere around the center of the energy gap may reduce the required energy leap by as much as half, making such generation more probable by several orders of magnitude. Since surface states typically form extremely wide bands that may extend over more than 1 eV, the probability of the surface excitation appears more likely. **Figure 6** shows, for example, a photoluminescence spectrum of In-Zn-O homologous superlattice nanowires. While the band-edge is lower by 0.1 eV relative to its typical position in ZnO, the sub-bandgap spectrum shows the classic sub-bandgap PL of ZnO: the so-called green luminescence band that spreads over ≈1.25 eV of the bandgap energy. The ZnO green luminescence has been positively identified to be a surface

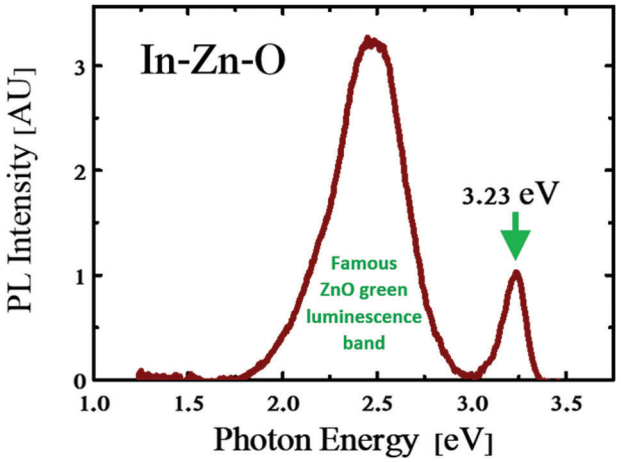

Figure 6. Photoluminescence obtained from In-Zn-O homologous superlattice nanowires. Compared with ZnO, the band-edge is redshifted by 0.1 eV. However at sub-bandgap energies, the famous ZnO green luminescence band, known to be a surface state [see Ref. [67] and references therein], spreads over a range as wide as 1.25 eV. This is not surprizing, as the main surface area of the wire is that of the ZnO sections.

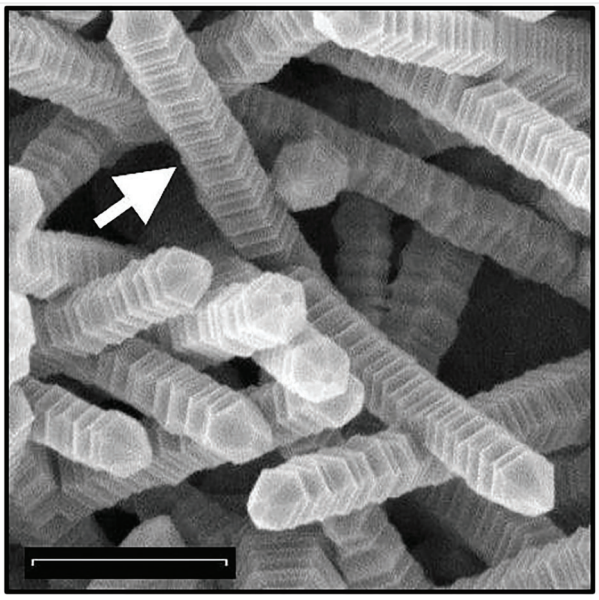

Figure 7. Data point 9 in Table 1 was obtained from this SEM image from the wire pointed at by the arrow. The scale bar is 1 μm long.

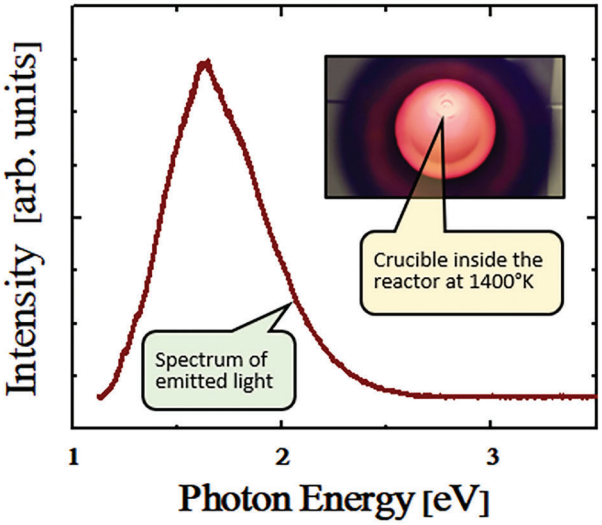

Figure 8. Spectrum of light emitted from the hot spot in the crystal growth reactor at a growth temperature of 1400 °K (an inset shows an optical image of the hot spot during the spectral acuisition). The spectrum peaks at ≈1.7 eV which is about half the bandgap of ZnO. The intensity subsides to zero well below the ultraviolet.

state (see, for example, ref. [68] and references therein). Hence, it is reasonable to expect that $G_B \ll G_S$. In such case, one may omit the bulk generation term from Equation (1), and obtain the following linear dependence of the section length on the nanowire diameter

$$L\ (R) = \frac{C}{2G_S}\ R \tag{3}$$

4. Experimental Section

To test the model, superlattice nanowire data were used that were collected from the literature. This was because our own data were found to span only a small part of the radius range reported in the literature. The preference was not to use numbers provided by authors but rather to assess all the data from the published electron microscopy images. To be included in the statistics, both the length of the section/period and the radius of the wire had to be unambiguously definable from electron microscope images.

The 9th data point for ZnO periodic lattice (without additional metal) was obtained from nanowires (**Figure 7**) grown by chemical vapor deposition on Si(111) wafers from a source (mixture of ZnO and graphite powders with indium metal) held at 1030 °C, while the substrate was held downstream at a point where the temperature was 950 °C. The growth was carried out under a flow of 30 sccm of Ar and lasted 30 min.

5. Results and Discussion

The availability of visible light photons emitted from the hot part of the reactor was tested by measuring the spectrum of the emitted light from the hot spot. **Figure 8** shows the acquired light emission spectrum at a growth temperature of 1400 °K peaking at about the center of the ZnO bandgap (≈1.7 eV). These observed photon energies are more than enough to support the proposed mechanism.

Table 1. Period (section length) and radius data of superlattice M-Zn-O nanowires collected from the literature.

Data	*M*	*L* [nm]	*R* [nm]	$L/R^{a)}$	Refs.
1	In, Sn	1.9	25	0.076	[40]
2	In, Al	3.2	27.3	0.117	[83]
3	In	3.3	37.5	0.088	[49]
4	Sn	4.0	34.3	0.117	[37]
5	In	4.5	52	0.087	[39]
6	In, Al	4.7	19.3	0.244	[83]
7	In, Al	6.6	64.5	0.102	[83]
8	In	7.3	61.5	0.119	[47]
9	In	23	155	0.143	This work
10	None	29	270	0.107	[68]

[a)] L-R correlation = 0.97.

We were able to find 10 such data points of M-Zn-O superlattice nanowires that met our selection criteria. The data and sources are listed in **Table 1**. SEM image of the wires used for data point 9 is shown in Figure 7. The 10th data point in Table 1 is a case of periodic twinning of ZnO. In that case, the same periodic structure was formed without intentional addition of another metal. Correlation of 0.97 calculated between the period, L, and the radius, R, for these data, corroborates our hypothesis of causative connection between the two parameters. Fit of these data with Equation (2) yielded a ratio $G_S/G_B \cong 10^{14}$ as predicted, meaning that the net generation in the bulk was extremely negligible (practically zero) compared to generation at the surface. We, therefore, replaced Equations (2) with (3).

Figure 9 plots the period, L, as a function of the radius, R, for the data of Table 1, and the fitting curve calculated using

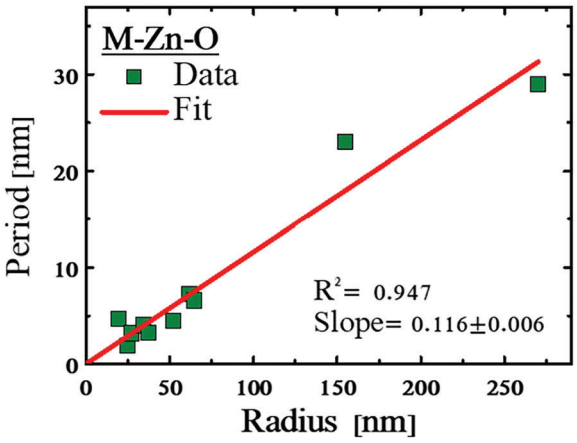

Figure 9. Period length as a function of wire radius for M-Zn-O superlattice wires which data are given in Table 1 (green squares) and a fitting curve obtained using using Equation (3) (red line). It should be emphasized that the data were collected from the literature from various studies and growth carried out under different conditions, but their variance is nonetheless excellent.

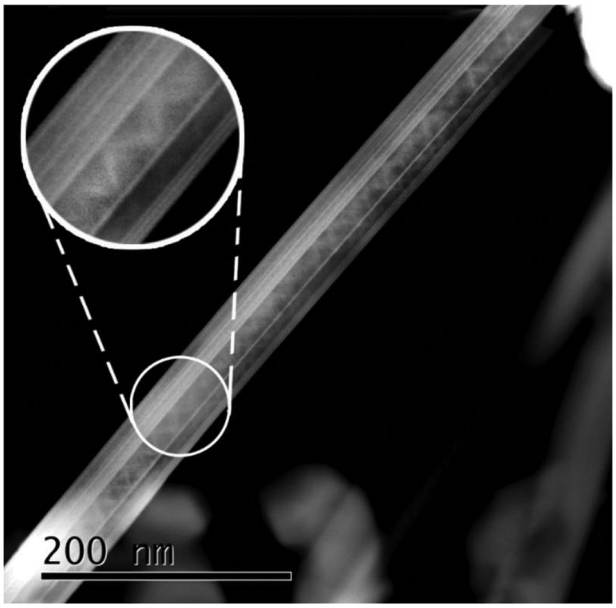

Figure 10. In-Zn-O wire wherein the periodicity is across the wire. The inset magnifies a portion of the wire showing the zigzag domain inversion boundary as commonly observed in the In-Zn-O structures.

Equation (3). The calculated coefficient of determination, R^2, for the fit is 0.95. This high value suggests that our model provides a fair description of the underlying physics: Our self-assembly mechanism is enabled by the presence of a special type of surface states. The formation of surface states is never uniform. Their typically high nonuniformity would imply a significant variance in period length in wires of the same growth run, same diameter, and even within a single wire. Indeed, this variance is commonly observed and has been reported in many papers.

There is, however, another observation in these superlattice nanowires that, at face value, appears to contradict our model. The same periodic structure, that we were able to explain when the periodicity is along the wire, is often observed across the wire (**Figure 10**). The polar axis "c" of the material is still parallel to the direction of the period, but the wire grows along the nonpolar axis "a." This may be straightforwardly explained, if we consider the fact that any growth starts from a nucleus. The nucleus may be viewed as a very short nanowire that develops in the same process proposed in our model. However, further growth takes place in the "a" direction using the nucleus as a template and thus extending the periodic structure sideways.

The same mechanism may also be at work in the case of layers. At the nuclei formation stage, there is practically no difference between a layer and a nanowire. The nuclei develop like small nanowires and then extend laterally keeping the vertical periodicity of the nuclei. However, since the periodicity may fluctuate, the resulting layer should be polycrystalline. Indeed, layers reported in the literature have all been polycrystalline. Small grains with high surface to volume ratio are also compatible with the premise of surface-state-assisted generation that we propose to be the source of electrical charge driving the periodic inversion. Hence, the same model may also explain the formation of superlattice-structured grains in ceramic polycrystalline layers and may also explain why the phenomenon has not been observed in large single crystals.

6. Conclusion

While much scientific and technological effort is devoted today to bandgap engineering of complicated heterostructures, nature appears to be able to carry out this task seamlessly and effortlessly in the formation of the homologous superlattices. Reviewing the literature, we have seen that intensive efforts to understand the formation of these structures have led to understanding of various subtle details of the structure. However, there has not been a single attempt to explain the formation of the periodic polarity switching which underlies the self-assembly.

In contrast, evidence has been accumulating that the wurtzite structure is predisposed to be affected by extrinsic electric fields because of its natural built-in polar field. To reach from there to the modeling of our self-assembly process requires only the realization of the fact that the main constituent of the homologous superlattices is a wurtzite material, ZnO, having a high spontaneous polarization. Once a strong built-in field is at work, optical generation of electron–hole pairs can produce charging and an external field to flip over the polarity. Hence, the homologous superlattice self-assembly may not be more than another example, albeit complicated, of the way wurtzite crystals respond to electrostatic phenomena during their growth.

Acknowledgements

The authors gratefully acknowledged the support of BSF Grant No. 2015700 and NSF Grant No. ECCS-1610362.

Conflict of Interest

The authors declare no conflict of interest.

Data Availability Statement

The data that support the findings of this study are available from the corresponding author upon reasonable request.

Keywords

crystal growth, electrostatics, self-assembly, semiconductors

Received: March 30, 2023
Revised: May 19, 2023
Published online: November 10, 2023

[1] Y. Ohya, T. Niwa, T. Ban, Y. Takahashi, *Jpn. J. Appl. Phys., Part 1* **2001**, *40*, 297.
[2] B. A. Haskell, S. J. Souri, M. A. Helfand, *J. Am. Ceram. Soc.* **1999**, *82*, 2106.
[3] P. F. Carcia, R. S. McLean, M. H. Reilly, G. Nunes, *Appl. Phys. Lett.* **2003**, *82*, 1117.
[4] E. M. C. Fortunato, P. M. C. Barquinha, A. C. M. B. G. Pimentel, A. M. F. Gonçalves, A. J. S. Marques, R. F. P. Martins, L. M. N. Pereira, *Appl. Phys. Lett.* **2004**, *85*, 2541.
[5] C. Wang, X. Chu, M. Wu, *Sens. Actuators, B* **2006**, *113*, 320.
[6] Ü. Özgür, Y. I. Alivov, C. Liu, A. Teke, M. A. Reshchikov, S. Doğan, V. Avrutin, S. J. Cho, H. Morkoç, *J. Appl. Phys.* **2005**, *98*, 041301.
[7] T. Minami, T. Kakumu, S. Takata, *J. Vac. Sci. Technol., A* **1996**, *14*, 1704.
[8] A. Wang, J. Dai, J. Cheng, M. P. Chudzik, T. J. Marks, R. P. H. Chang, C. R. Kannewurf, *Appl. Phys. Lett.* **1998**, *73*, 327.
[9] H. K. Hideo Hosono, M. Yasakawa, *J. Non-Cryst. Solids* **1996**, *203*, 334.
[10] C. Li, Y. Bando, M. Nakamura, N. Kimizuka, *J. Electron. Microsc.* **1997**, *46*, 119.
[11] H. Ohta, K. Nomura, M. Orita, M. Hirano, K. Ueda, T. Suzuki, Y. Ikuhara, H. Hosono, *Adv. Funct. Mater.* **2003**, *13*, 139.
[12] S. Liang, H. Sheng, Y. Liu, Z. Huo, Y. Lu, H. Shen, *J. Cryst. Growth* **2001**, *225*, 110.
[13] K. Nomura, H. Ohta, K. Ueda, T. Kamiya, M. Hirano, H. Hosono, *Science* **2003**, *300*, 1269.
[14] K. Nomura, H. Ohta, A. Takagi, T. Kamiya, M. Hirano, H. Hosono, *Nature* **2004**, *432*, 488.
[15] K. Nomura, T. Kamiya, H. Ohta, K. Ueda, M. Hirano, H. Hosono, *Appl. Phys. Lett.* **2004**, *85*, 1993.
[16] N. L. Dehuff, E. S. Kettenring, D. Hong, H. Q. Chiang, J. F. Wager, R. L. Hoffman, C. H. Park, D. A. Keszler, *J. Appl. Phys.* **2005**, *97*, 064505.
[17] H. S. Choi, S. Jeon, H. Kim, J. Shin, C. Kim, U. I. Chung, *Appl. Phys. Lett.* **2012**, *100*, 173501.
[18] J. Jeong, J. Kim, G. J. Lee, B. D. Choi, *Appl. Phys. Lett.* **2012**, *100*, 023506.
[19] M. Fujii, Y. Ishikawa, R. Ishihara, J. Van Der Cingel, M. R. T. Mofrad, M. Horita, Y. Uraoka, *Appl. Phys. Lett.* **2013**, *102*, 122107.
[20] W. B. Jackson, R. L. Hoffman, G. S. Herman, *Appl. Phys. Lett.* **2005**, *87*, 193503.
[21] H. Q. Chiang, J. F. Wager, R. L. Hoffman, J. Jeong, D. A. Keszler, *Appl. Phys. Lett.* **2005**, *86*, 2003.
[22] J. K. Jeong, H. Won Yang, J. H. Jeong, Y. G. Mo, H. D. Kim, *Appl. Phys. Lett.* **2008**, *93*, 8.
[23] P. Barquinha, A. Vila, G. Gonçalves, L. Pereira, R. Martins, J. Morante, E. Fortunato, *Phys. Status Solidi A* **2008**, *205*, 1905.
[24] X. Huang, C. Wu, H. Lu, F. Ren, Q. Xu, H. Ou, R. Zhang, Y. Zheng, *Appl. Phys. Lett.* **2012**, *100*, 243505.
[25] S. Kim, K. K. Kim, H. Kim, *Appl. Phys. Lett.* **2012**, *101*, 033506.
[26] Z. Lou, L. Li, G. Shen, *Adv. Electron. Mater.* **2015**, *1*, 1500054.
[27] C. H. Ahn, K. Senthil, H. K. Cho, S. Y. Lee, *Sci. Rep.* **2013**, *3*, 2737.
[28] A. Kudo, I. Mikami, *Chem. Lett.* **1998**, *27*, 1027.
[29] J. G. Lu, P. Chang, Z. Fan, *Mater. Sci. Eng., R* **2006**, *52*, 49.
[30] V. H. Kasper, *Z. Anorg. Allg. Chem.* **1967**, *349*, 113.
[31] P. J. Cannard, R. J. D. Tilley, *J. Solid State Chem.* **1988**, *73*, 418.
[32] M. Nakamura, N. Kimizuka, T. Mohri, *J. Solid State Chem.* **1991**, *93*, 298.
[33] C. Schinzer, F. Heyd, S. F. Matar, *J. Mater. Chem.* **1999**, *9*, 1569.
[34] C. Li, Y. Bando, M. Nakamura, M. Onoda, N. Kimizuka, *J. Solid State Chem.* **1998**, *139*, 347.
[35] Y. Michiue, N. Kimizuka, *Acta Crystallogr.* **2010**, *B66*, 117.
[36] K. Park, K. K. Kim, N. Lee, S. J. Kim, *J. Kor. Phys. Soc.* **2006**, *49*, 1548.
[37] B. Cao, T. Shi, S. Zheng, Y. H. Ikuhara, W. Zhou, D. Wood, M. Al-Jassim, Y. Yan, *J. Phys. Chem. C* **2012**, *116*, 5009.
[38] Y. Yan, S. J. Pennycook, J. Dai, R. P. H. Chang, A. Wang, T. J. Marks, *Appl. Phys. Lett.* **1998**, *73*, 2585.
[39] J. Jie, G. Wang, X. Han, J. G. Hou, *J. Phys. Chem. B* **2004**, *108*, 17027.
[40] C. W. Na, S. Y. Bae, J. Park, *J. Phys. Chem. B* **2005**, *109*, 12785.
[41] L. Xu, Y. Su, Y. Chen, H. Xiao, L. A. Zhu, Q. Zhou, S. Li, *J. Phys. Chem. B* **2006**, *110*, 6637.
[42] H. Duan, H. He, L. Sun, S. Song, Z. Ye, *Nanoscale Res. Lett.* **2013**, *8*, 493.
[43] S. Y. Bae, C. W. Na, J. H. Kang, J. Park, *J. Phys. Chem. B* **2005**, *109*, 2526.
[44] C.-L. Hsu, S.-J. Chang, Y.-R. Lin, J.-M. Wu, T.-S. Lin, S.-Y. Tsai, I.-C. Chen, *Nanotechnology* **2006**, *17*, 516.
[45] L. Xu, Y. Su, Y. Chen, H. Xiao, L. Zhu, Q. Zhou, S. Li, *J. Phys. Chem. B* **2006**, *110*, 6637.
[46] L. Wu, X. Zhang, Z. Wang, Y. Liang, H. Xu, *J. Phys. D: Appl. Phys.* **2008**, *41*, 195406.
[47] X. Zhang, H. Lu, H. Gao, X. Wang, H. Xu, Q. Li, S. Hark, *Cryst. Growth Des.* **2009**, *9*, 364.
[48] M. Ahmad, J. Zhao, J. Iqbal, W. Miao, L. Xie, R. Mo, J. Zhu, *J. Phys. D: Appl. Phys.* **2009**, *42*, 165406.
[49] B. Niu, L. Wu, X. Zhang, *CrystEngComm* **2010**, *12*, 3305.
[50] R. Yousefi, M. R. Muhamad, A. K. Zak, *Thin Solid Films* **2010**, *518*, 5971.
[51] R. Yousefi, F. Jamali-Sheini, A. Khorsand-Zak, M. Azarang, *Ceram. Internat.* **2013**, *39*, 5191.
[52] S. Y. Lim, S. Brahma, C.-P. Liu, R.-C. Wang, J.-L. Huang, *Thin Solid Films* **2013**, *549*, 165.
[53] S. Farid, S. Mukherjee, K. Sarkar, M. Mazouchi, M. A. Stroscio, M. Dutta, *Appl. Phys. Lett.* **2016**, *108*, 021106.
[54] J. Jie, G. Wang, X. Han, Q. Yu, Y. Liao, G. Li, J. G. Hou, *Chem. Phys. Lett.* **2004**, *387*, 466.
[55] P. X. Gao, Y. Ding, W. Mai, W. L. Hughes, C. Lao, Z. L. Wang, *Science* **2005**, *309*, 1700.
[56] B. Alemán, P. Fernández, J. Piqueras, *Appl. Phys. Lett.* **2009**, *95*, 013111.
[57] D. P. Li, G. Z. Wang, X. H. Han, J. S. Jie, S. T. Lee, *J. Phys. Chem. C* **2009**, *113*, 5417.
[58] D. P. Li, G. Z. Wang, X. H. Han, *J. Phys. D: Appl. Phys.* **2009**, *42*, 175308.
[59] L. L. Wu, Y. Liang, F. W. Liu, H. Q. Lu, H. Y. Xu, X. T. Zhang, S. Hark, *CrystEngComm* **2010**, *12*, 4152.
[60] J. Y. Zhang, Y. Lang, Z. Q. Chu, X. Liu, L. L. Wu, X. T. Zhang, *CrystEngComm* **2011**, *13*, 3569.
[61] H. J. Fan, B. Fuhrmann, R. Scholz, C. Himcinschi, A. Berger, H. Leipner, A. Dadgar, A. Krost, S. Christiansen, U. Gösele, M. Zacharias, *Nanotechnology* **2006**, *17*, S231.
[62] C. Xia, R. Asahi, T. Tani, *J. Cryst. Growth* **2003**, *254*, 144.
[63] H. Gao, H. Ji, X. Zhang, H. Lu, Y. Liang, *J. Vac. Sci. Tech. B* **2008**, *26*, 585.

[64] M. N. Jung, E. S. Lee, T.-I. Jeon, K. S. Gil, J. J. Kim, Y. Murakami, S. H. Lee, S. H. Park, H. J. Lee, T. Yao, H. Makino, J. H. Chang, *J. Alloys Comp.* **2009**, *481*, 649.
[65] K. Mahmood, S. B. Park, H. J. Sung, *J. Mater. Chem. C* **2013**, *1*, 3138.
[66] T. Moriga, D. D. Edwards, T. O. Mason, G. B. Palmer, K. R. Poeppelmeier, J. L. Schindler, C. R. Kannewurf, I. Nakabayashi, *J. Am. Ceram. Soc.* **1998**, *81*, 1310.
[67] M. Lopez-Ponce, A. Nakamura, M. Suzuki, J. Temmyo, S. Agouram, M. C. Martínez-Tomás, V. Muñoz-Sanjosé, P. Lefebvre, J. M. Ulloa, E. Muñoz, A. Hierro, *Nanotechnology* **2014**, *25*, 255202.
[68] I. Shalish, H. Temkin, V. Narayanamurti, *Phys. Rev. B* **2004**, *69*, 245401.
[69] Y. Hao, G. Meng, Z. L. Wang, C. Ye, L. Zhang, *Nano Lett.* **2006**, *6*, 1650.
[70] D.-H. Wang, D. Xu, Q. Wang, Y.-J. Hao, G.-Q. Jin, X.-Y. Guo, K. N. Tu, *Nanotechnology* **2008**, *19*, 215602.
[71] H. W. Shim, Y. Zhang, H. Huang, *J. Appl. Phys.* **2008**, *104*, 063511.
[72] Y. Yan, J. L. F. Da Silva, S.-H. Wei, M. Al-Jassim, *Appl. Phys. Lett.* **2007**, *90*, 261904.
[73] S. Yoshioka, K. Toyoura, F. Oba, A. Kuwabara, K. Matsunaga, I. Tanaka, *J. Solid State Chem.* **2008**, *181*, 137.
[74] J. L. F. Da Silva, Y. Yan, S.-H. Wei, *Phys. Rev. Lett.* **2008**, *100*, 255501.
[75] J. L. F. Da Silva, A. Walsh, S.-H. Wei, *Phys. Rev. B* **2009**, *80*, 214118.
[76] F. Röder, A. Lubk, H. Lichte, T. Bredow, W. Yu, W. Mader, *Ultramicroscopy* **2010**, *110*, 400.
[77] J. Wen, X. Zhang, H. Gao, *J. Solid State Chem.* **2015**, *222*, 25.
[78] A. R. Azulay, Y. Turkulets, D. Del Gaudio, R. S. Goldman, I. Shalish, *Sci. Rep.* **2020**, *10*, 6554.
[79] Y. Turkulets, I. Shalish, *Phys. Rev. Mater.* **2019**, *3*, 033403.
[80] X. Hou, K. L. Choy, *Chem. Vap. Depos.* **2006**, *12*, 631.
[81] M. A. Reshchikov, J. D. McNamara, H. Helava, A. Usiko, Y. Makarov, *Sci. Rep.* **2018**, *8*, 8091.
[82] L. Esaki, R. Tsu, *IBM J. Res. Dev.* **1970**, *14*, 61.
[83] D. L. Huang, L. L. Wu, X. T. Zhang, *J. Phys. Chem. C* **2010**, *114*, 11783.